JOURNAL OF Materials CHEMISTRY

Growth by laser ablation of Y_2O_3 and $Tm:Y_2O_3$ thin films for optical applications

Arnaud Huignard,[a,b] Astrid Aron,[a] Patrick Aschehoug,[a] Bruno Viana,[a] Jeanine Théry,[a] Alain Laurent[b] and Jacques Perrière*[b]

[a]*Laboratoire de Chimie Appliquée de l'Etat Solide, CNRS UMR 7574, ENSCP, 11 rue Pierre et Marie Curie, 75231 Paris Cédex 05, France*
[b]*Groupe de Physique des Solides, Universités Paris VI et Paris VII, CNRS UMR 7588, 2 Place Jussieu, 75251 Paris Cédex 05, France*

Received 14th June 1999, Accepted 3rd December 1999

Crystalline undoped and thulium doped yttrium oxide (Y_2O_3) thin films have been grown by the pulsed laser deposition (PLD) technique on various single-crystal substrates heated at 700 °C. X-Ray diffraction (XRD) analysis showed that the orientations of the films depended on the substrate and on the oxygen pressure. The crystalline quality of Y_2O_3 thin films, studied by rocking-curve measurements and by Rutherford backscattering spectroscopy (RBS) in channeling geometry, and the in-plane orientations between films and substrates, determined by X-ray asymmetric diffraction, were also found to depend on the same parameters. The recording of the visible fluorescence spectra of the thulium (Tm) doped Y_2O_3 thin films, as well as the measurements of the fluorescence lifetimes of the $^1D_2$ and $^1G_4$ thulium emitting levels, gave results very similar to those obtained on bulk crystals. Doping rates in Tm of 0.5 and 1% were found to limit Tm–Tm interactions inside the films and to give relatively high visible fluorescence intensities.

Introduction

The growth of crystalline thin films for optical applications, such as phosphors or laser waveguides, has recently attracted much attention. Among other materials, doped yttrium oxide is a good candidate for such optical applications. Y_2O_3 presents a high thermal conductivity ($k = 0.33$ W cm^{-1} K^{-1}), superior to that of YAG ($k = 0.13$ W cm^{-1} K^{-1}), a large transparency range (0.23–8 μm)[1] and a relatively high refractive index (1.9) which is well suited for waveguide applications. Moreover, Y_2O_3, which has a bixbyite type crystal structure similar to fluorite with 25% of oxygen vacancies along the [111] direction, is a well known host matrix for rare-earth ions. Unfortunately, the crystalline growth of bulk Y_2O_3 is very difficult given the high melting point of this material ($T_m = 2450$ °C). Therefore, it is desirable to grow Y_2O_3 as thin films.

Several methods have been used for this purpose, such as electron-beam evaporation,[2] radio frequency sputtering[3,4] or reactive ionized cluster beam deposition.[5] Pulsed laser deposition (PLD), which is a popular method to grow thin oxide films of complex compositions, has also been recently used and seems to be well adapted to the growth of Y_2O_3,[6] as well as Eu doped Y_2O_3.[7–9]

Here, we report on the pulsed laser deposition of undoped and thulium doped yttrium oxide crystalline thin films on single crystal substrates such as yttria stabilized zirconia (YSZ), magnesium oxide (MgO) and silicon (Si). The purpose of this study is twofold. First, it is to determine the influence of the experimental conditions (substrate, oxygen pressure) on the growth of Y_2O_3 crystalline thin films. The second purpose is to assess the optical properties (luminescence) of Tm doped Y_2O_3 thin films. The choice of the active species, thulium, is explained by the fact that bulk $Tm:Y_2O_3$ crystals exhibit luminescence in both the visible and IR domains and presents a laser effect at 1.95 μm, due to the $^3F_4 \rightarrow {}^3H_6$ transition of the Tm^{3+} ions.[10] This latter point is very interesting in view of laser waveguide applications.

Experimental

Thin films of Y_2O_3 were grown onto Si(100), MgO(100) and YSZ(100) single crystals (*ca.* 1 cm^2 surface area). The details of PLD methods are given elsewhere.[11] Briefly, the laser was a Nd:YAG (supplied by BMI), delivering pulses of 5 ns duration at a rate of 5 Hz. The films were grown at the fourth harmonic wavelength (266 nm), which was generated by frequency doubling KDP crystals. The available laser intensity at the surface was typically in the range 50–300 MW cm^{-2}. The *in situ* growth of the films was achieved by deposition onto heated substrates (700 °C) under various oxygen pressures (from 10^{-6} to 0.5 mbar). The targets used in this work were sintered pellets of undoped Y_2O_3 or 3%, 1% and 0.5% Tm doped Y_2O_3, corresponding to the compositions $Y_{1.94}Tm_{0.06}O_3$, $Y_{1.98}Tm_{0.02}O_3$ and $Y_{1.99}Tm_{0.01}O_3$. For the undoped targets, the Y_2O_3 powder was pressed and sintered in air for 48 h at 1600 °C. For the Tm doped Y_2O_3 targets, the Tm_2O_3 and Y_2O_3 powders were mixed together in the appropriate proportions, pressed and heated in air at 1300 °C for 48 h. After grinding, mixing and pressing, reaction sintering was achieved in air at 1600 °C for 48 h.

UV–VIS absorption spectra of the targets were measured with a Varian Cary 5 spectrophotometer in diffuse reflectance geometry. This was performed to detect both the absorption of Y_2O_3 at 266 nm and the thulium transitions in the Y_2O_3 matrix. The crystalline orientations of the films were determined using a Siemens D-5000 diffractometer using Co-Kα radiation ($\lambda = 1.789$ Å), which gave both θ–2θ diagrams and rocking curves. The in-plane orientations of the films were studied by asymmetric diffraction ('ϕ-scan' measurements), using a Philips X-Pert diffractometer with Cu-Kα radiation ($\lambda = 1.540$ Å). The composition and thickness of the films were determined by Rutherford backscattering spectroscopy (RBS). The RBS experiments were carried out using a $^4He^+$ ion beam from a 2.5 MeV van de Graaff accelerator. The visible luminescence properties of the films were investigated at room temperature.

The excitation wavelength was 355 nm, which corresponds to the third harmonic of a Nd : YAG laser. An optical grating and a photodiode linear array (Optical Multichannel Analyser) were used, to disperse and collect the emitted light, respectively.

Results and discussion

Growth of undoped Y_2O_3 films

It has been found that the surface morphology of the the films depends on the optical properties of the target.[12] The higher the optical absorption coefficient the lower the droplet density at the surface of the films. The absorption coefficient of Y_2O_3 at 266 nm, the wavelength used for the deposition, was found to be high and, therefore, no droplets could be observed by scanning electron microscopy at the surface of the Y_2O_3 thin films. Such a smooth surface is well suited for waveguide applications.

A typical RBS spectrum for a film grown on Si under vacuum is shown in Fig. 1. The calculated spectrum using the RUMP simulation,[13] corresponding to a composition $Y_2O_{2.8}$ and a thickness of 0.3 μm, is also shown. The slight oxygen deficiency, only observed under vacuum, whatever the substrate in similar growth conditions, is certainly due to the growth rate. We also grew films on Si at a ten times lower growth rate. Under these conditions, obtained by reducing the usual fluence of the laser, the films were stoichiometric.

At the deposition temperature (700 °C), the Y_2O_3 thin films were crystalline and textured. However, the orientations were found to depend on the substrates and on the oxygen pressure, as shown in Table 1.

For depositions on Si(100) under vacuum, the films were highly textured along the [111] direction. An extremely sharp and intense peak, corresponding to the (222) reflection of cubic Y_2O_3, was observed for the X-ray diffraction (XRD) pattern shown in Fig. 2. The XRD patterns from films grown on MgO(100) at different oxygen pressures are shown in Fig. 3. For oxygen pressures of <0.1 mbar, the film orientation was (111). The major peak, which was attributed to the (222) reflection of cubic yttrium oxide, is associated with a *d*-spacing of 3.080 Å, whereas for Y_2O_3 targets, as well as Y_2O_3 films grown on Si(100) under vacuum, the *d*-spacing of the (222) reflection is 3.062 Å. For oxygen pressures of >0.1 mbar, the film orientation changed to a mixture of (111) and (100) orientations. Meanwhile, the *d*-spacing of the (222) ray tended to 3.062 Å. Fig. 4 shows XRD patterns from films grown on YSZ(100) at different oxygen pressures. Under vacuum, the films were textured along the [100] direction. For oxygen

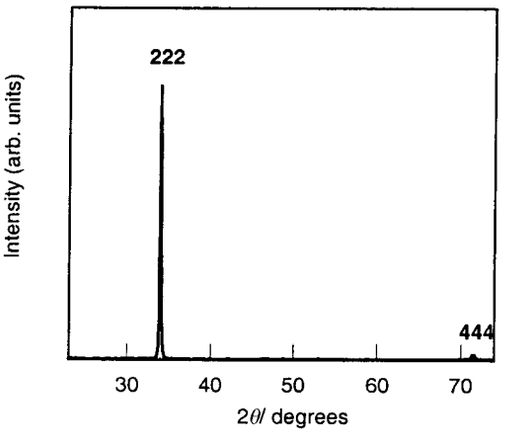

Fig. 2 XRD pattern of a Y_2O_3 thin film grown on Si(100) under vacuum.

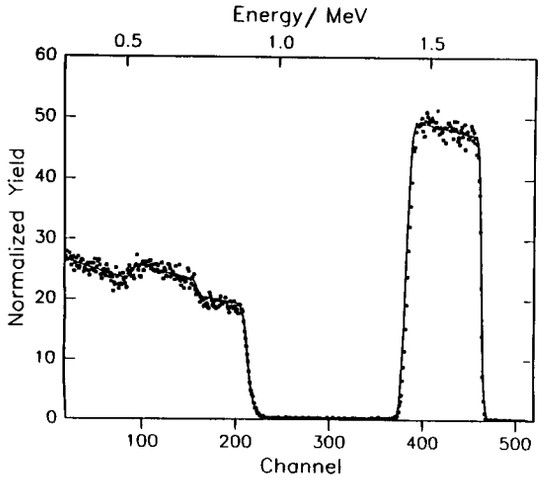

Fig. 1 RBS spectrum for a Y_2O_3 thin film deposited on Si(100). The solid line is the calculated RUMP spectrum.

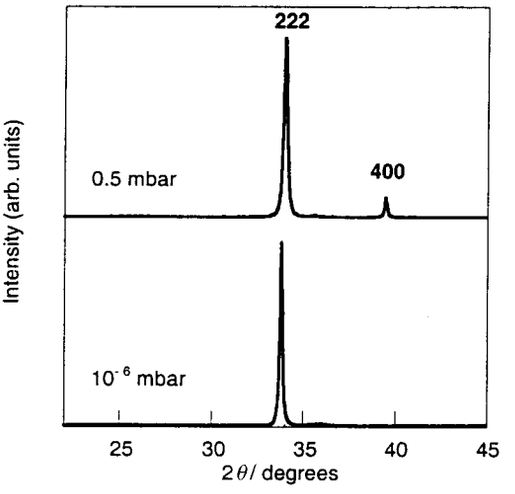

Fig. 3 XRD patterns of Y_2O_3 thin films grown on MgO(100) under different oxygen pressures.

Table 1 Role of substrate and oxygen pressure on the orientations and the crystalline quality of Y_2O_3 thin films

Substrate	Oxygen pressure/ mbar	Orientation	Rocking curve (FWHM/°)	χ_{min} (RBS) (%)
Si(100)	10^{-6}	(111)	2.3	>90
MgO(100)	10^{-6}	(111)	1.3	70
	0.1	(111)	1.4	70
		(100)	—	
	0.5	(111)	1.6	—
		(100)	3.7	
YSZ(100)	10^{-6}	(100)	0.6	5
	0.01	(100)	1.5	70
		(111)	—	

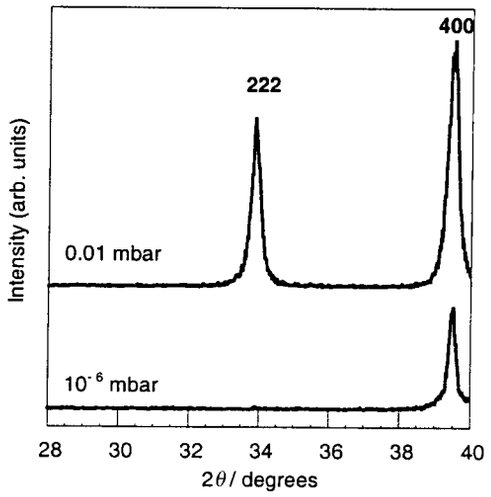

Fig. 4 XRD patterns of Y_2O_3 thin films grown on YSZ under different oxygen pressures.

pressures >0.01 mbar, the films presented a mixture of (100) and (111) orientations.

These orientations of the films are believed to depend on several factors, among others, the film surface free energy and the lattice mismatch between film and substrate. On Si(100) and MgO(100), the prevailing factor seems to be the film surface free energy. As in cubic Y_2O_3 the (111) surface of the film has the lowest surface free energy,[6,7] and growth along this orientation is preferential, especially on substrates which do not present a low lattice mismatch with the film. On silicon substrates, as no special treatment is performed before the depositions, a film of amorphous silica is present at the surface. As a consequence, the crystallinity of Si(100) is not sufficient to induce the growth along the (100) orientation and the effect of the substrate appears to be low. On MgO(100), the situation is different. In the (100) crystalline planes of MgO, Y_2O_3 films can grow either along the [100] axis or along the [110] axis (Fig. 5). The lattice mismatches for these different possible growths are shown in Table 2. The lowest lattice mismatches are observed for the growth of (100) Y_2O_3 films along the [100] axis of MgO and (111) Y_2O_3 films along the [110] axis of MgO. However, as they are equal, MgO substrates do not favour either of the two orientations of the Y_2O_3 films. The prevailing factor then appears to be the surface free energy, which leads to a preferential growth along the [111] direction. However, in contrast to Si(100), MgO substrates have an effect on the growth of the films as shown by the *d*-spacing of the (222) reflection which shows that growth on MgO(100) is

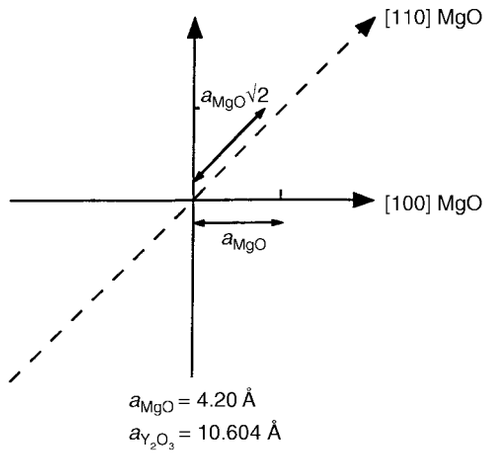

Fig. 5 Possible growths of Y_2O_3 films in the MgO(100) plane.

Table 2 Lattice mismatches for (111) Y_2O_3 and (100) Y_2O_3 in the (100) MgO plane

Y_2O_3 orientation	Lattice mismatch (%)
(100)	[100] 1.4
	[110] 12
(111)	[100] 5
	[110] 1.4

strained. The (100) orientation for films grown on YSZ(100) under vacuum can be explained by both the structural similarity and the low lattice mismatch between film and substrate. Indeed, YSZ has a fluorite type structure with a lattice parameter of 5.14 Å, whereas Y_2O_3 has a fluorite type structure with oxygen vacancies and a lattice parameter of 10.604 Å.

Concerning the change of orientations for growth under oxygen pressure on MgO and YSZ, a similar behaviour has been observed by Zhang and Xiao[6] and Jones *et al.*[7] for depositions of Y_2O_3 on Si. According to these studies, a change of film orientations is believed to be associated with an increase in the density of outgrowths on the surface with an increase in oxygen pressure. These outgrowths, which result from the enhanced probability of formation of clusters of ablated species in the laser plume under oxygen pressure, may act as nucleation centers for other orientations. This could explain the growths along the (100) orientation on MgO and (111) orientation on YSZ under oxygen pressure, orientations which are not observed under vacuum.

The crystalline quality of the films was studied by rocking-curve measurements, which determines the mosaicity of the films and by RBS in channeling geometry, which gives indications on defects in the crystalline domains (Fig. 6).

As shown in Table 1, the crystalline quality of the films depends on the substrate and on the oxygen pressure. For growth under vacuum, Si and MgO substrates give very similar results. A high mosaicity is observed, especially on Si, which indicates that the disorientation between the (111) domains is important. Inside these domains, the crystalline quality is low as shown by the χ_{min} measurements. However, it should be noted that the crystalline quality of the (111) domains can be improved on MgO(100) for lower growth rates. A χ_{min} of 13% was thus measured for a ten times lower growth rate than that described in this paper. This indicates a good crystalline quality of the (111) domains. The crystalline quality for films grown on YSZ(100) under vacuum is found to be far better. First, the mosaicity is dramatically reduced compared to Si and MgO substrates. Disorientation between the (100) domains exists but

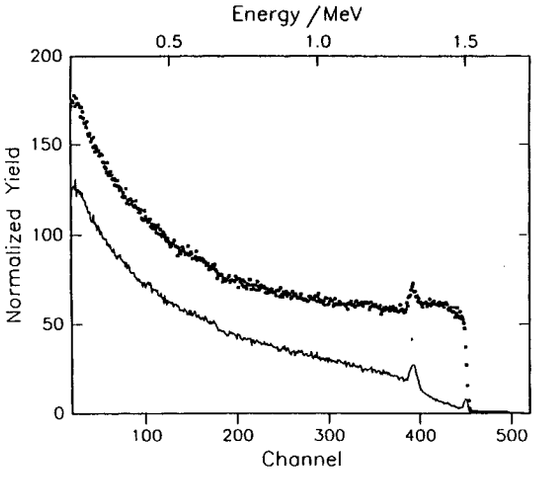

Fig. 6 RBS spectrum for a Y_2O_3 thin film deposited on YSZ(100) (700 °C, under vacuum) in channeling geometry.

Table 3 Role of substrate and oxygen pressure on the in-plane orientations of Y_2O_3 films

Substrate	Oxygen pressure/mbar	Domains	Epitaxial relationships	FWHM ϕ-scan/°
Si(100)	10^{-6}	(111)	—	—
MgO(100)	10^{-6}	(111)	$[10\bar{1}] \parallel [110]$	4
	0.5	(111)	$[10\bar{1}] \parallel [110]$	5.7
		(100)	$[100] \parallel [100]$	7
YSZ(100)	10^{-6}	(100)	$[100] \parallel [100]$	1.6
	0.5	(100)	$[100] \parallel [100]$	3.8
		(111)	—	—

is relatively low [disorientation of YSZ(100) = 0.25°]. Secondly, a χ_{min} of 5% was measured. For comparison, a typical value of χ_{min} for a bulk monocrystal is 2%. This means that the crystalline quality of the (100) domains of the Y_2O_3 films grown on YSZ (100) is very high.

For growth under oxygen pressure, the mosaicity of the Y_2O_3 films increases whereas the crystalline quality of the domains decreases, whatever the substrate (YSZ or MgO). This can be explained by the fact that in the presence of oxygen, the kinetic energy of the species is reduced, due to collisions between the ablated particles and the gas molecules. This lowers the mobility of the species when they are adsorbed on the surface of the film. The disorientation of the domains is then enhanced and the number of defects increases.

The study of the in-plane orientations by asymmetric diffraction allows one to determine the epitaxial relationships between films and substrates, but also gives indications on the quality of the epitaxy. Indeed, the FWHM of the 'ϕ-scans' corresponds to an angular disorientation of the domains in the plane of the substrate. Results relating to this study are summarized in Table 3.

The Y_2O_3 films grown on Si(100) did not present any in-plane orientation. This is certainly due to the silicon substrates which are covered by a slight film of amorphous silica. For films deposited on YSZ(100) under vacuum, the growth was epitaxial: the [100] directions are parallel to the [100] directions of the substrate. This result is a consequence of the fact that Y_2O_3 and YSZ show very similar structures and a low lattice mismatch along this direction. Moreover, the FWHM of the 'ϕ-scans' were relatively low, which indicates a good epitaxy of the (100) domains on YSZ(100). By contrast, for growths under oxygen pressure, the quality of the epitaxy of the (100) domains dramatically decreased. Meanwhile, the (111) domains, which also exist under these conditions, are not epitaxially grown. The 'ϕ-scan' from a film grown on MgO(100) under vacuum is shown in Fig. 7. It shows diffraction peaks every 30°, with a shift of 15° towards the [100] directions of MgO(100). The diffraction peaks however were very broad (Table 3). This can be explained by a preferential growth of the $Y_2O_3[10\bar{1}]$ directions parallel to the [110] directions of the substrate. Indeed, along these directions, the lattice mismatch is only 1.4% as calculated previously. For films grown under oxygen pressure, the FWHM of the 'ϕ-scans' of the (111) domains increased. Concerning the (100) domains, they were also preferentially grown in the MgO plane, corresponding to a cube on cube growth. However, the diffraction peaks were even broader than those recorded for the (111) domains under the same conditions.

Growth and optical properties of $Tm:Y_2O_3$ films

The thulium doped Y_2O_3 thin films were grown under vacuum and at a substrate temperature of 700 °C. These experimental conditions give highly textured films whatever the substrate, as described in the previous section. The insertion of thulium into the films does not change the properties observed for the undoped films under the same conditions, except for the crystalline quality which was found to decrease a little. For example, for a $Tm:Y_2O_3$ (3 atom%) film grown on YSZ(100), the χ_{min} was 12%, whereas it was only 5% for an undoped film.

RBS measurements showed that the atomic ratio of yttrium to thulium was exactly the same in the target and in the films. Therefore, PLD appears to be a very suitable method to grow thulium doped yttrium oxide thin films, with a very precise control of the doping rate.

Prior to the study of the emission of the thulium doped thin films, it was necessary to locate the absorption lines of thulium in the Y_2O_3 matrix. This was realized on the targets. The absorption spectrum of a 1% Tm doped Y_2O_3 target is shown in Fig. 8. The interesting transitions for optical pumping are $^3H_6 \rightarrow {}^1D_2$ ($\lambda = 355$ nm) to study visible luminescence and $^3H_6 \rightarrow {}^3H_4$ ($\lambda = 810$ nm) to study near-IR luminescence. Hence, we only report on the study of the visible luminescence of the Y_2O_3 thin films.

The excitation wavelength for the study of the visible luminescence of the $Tm:Y_2O_3$ thin films was $\lambda = 355$ nm, which corresponds to the $^3H_6 \rightarrow {}^1D_2$ transition. Luminescence spectra of a 1% Tm doped Y_2O_3 thin film grown on silicon are shown in Fig. 9. Several transitions due to the thulium ions in the yttrium

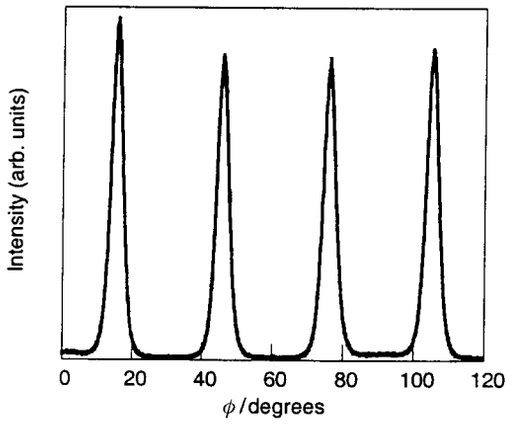

Fig. 7 'ϕ-scan' of a Y_2O_3 thin film grown on MgO(100) (700 °C, under vacuum).

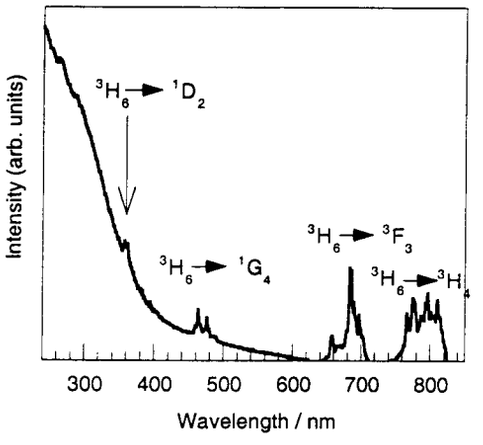

Fig. 8 Visible absorption spectrum of a Tm (1 atom%) : Y_2O_3 target.

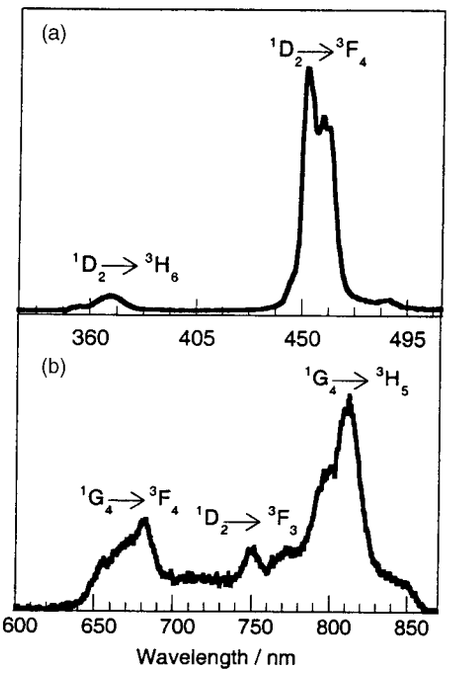

Fig. 9 Room temperature fluorescence spectra of a Tm (1 atom%) : Y_2O_3 thin film deposited on Si(100) under excitation in the $^1D_2$ energy level ($\lambda_{ex} = 355$ nm).

oxide matrix were observed. The most intense was the $^1D_2 \rightarrow {}^3F_4$ transition at a wavelength of 451 nm. These spectra were similar to those previously observed[1] for Tm doped Y_2O_3 crystalline fibers. The effect of the thulium concentration on the emission of the films was also studied. Tm doped Y_2O_3 films, containing 3%, 1% and 0.5% thulium ions, were grown on silicon. The luminescence spectra around 450 nm of the 1% and 0.5% thulium doped films are more intense than for the 3% thulium doped film. This qualitative information, which requires intensity measurements of the various films under the same geometrical conditions in front of the detector, was completed by a quantitative measurement of the fluorescence intensity decay profiles. Luminescence decay profiles of the $^1D_2 \rightarrow {}^3F_4$ transition at *ca.* 451 nm were measured for the three thulium ion concentrations (Fig. 10). For the 1% and 0.5% thulium doped films, the decays showed nearly exponential behavior with fairly long lifetimes of 6.5 μs and 7 μs, respectively. The 3% thulium doped film presents a non-exponential decay profile (see Fig. 10) but at longer times an exponential region could be measured with a lifetime of 3.3 μs.

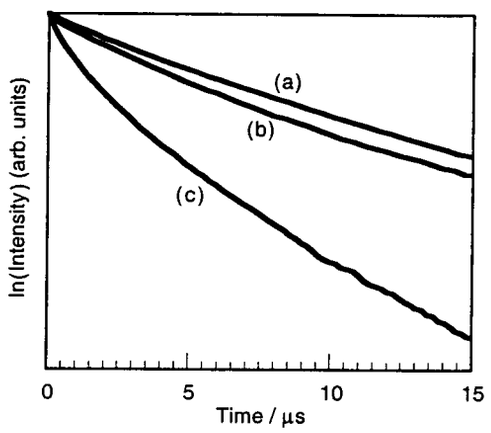

Fig. 10 $^1D_2$ fluorescence decay profiles at *ca.* 450 nm in Tm (x atom%) : Y_2O_3 thin films with (a) $x = 0.5\%$, (b) $x = 1\%$, (c) $x = 3\%$ ($\lambda_{ex} = 355$ nm and $T = 300$ K).

Table 4 Fluorescence lifetimes for various Tm : Y_2O_3 films grown on silicon

Tm concentration (atom%)	$\tau(^1D_2)$/μs	$\tau(^1G_4)$/μs
3	3.3	20
1	5.5	90
0.5	6.5	200

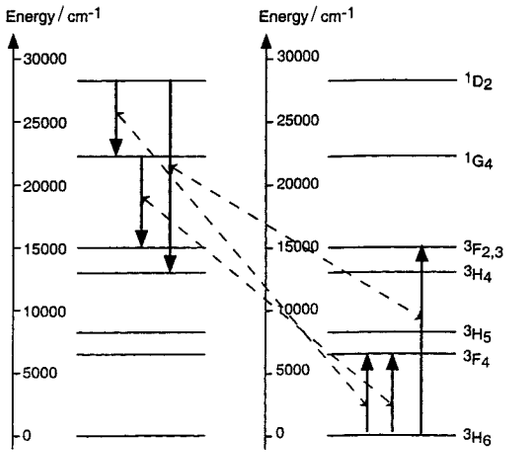

Fig. 11 Possible cross-relaxation mechanisms from the $^1D_2$ and $^1G_4$ thulium emitting levels.

The intensity decay profiles for the three different thulium concentrations were also measured for the $^1G_4$ emitting level. The same non-exponential behavior as for the $^1D_2$ level was observed along with a decrease of the lifetime values for higher thulium concentrations. These results, which were in full accord with those observed for bulk Tm : Y_2O_3 crystals,[1,14] are gathered in Table 4. Here, the reported lifetimes correspond to the exponential profiles at longer times.

The measurements of the luminescence decay profiles of the $^1D_2 \rightarrow {}^3F_4$ transition and the variation of the lifetimes of the $^1D_2$ and $^1G_4$ emitting levels show the existence of Tm–Tm interactions inside the Tm : Y_2O_3 films. Cross relaxation mechanisms represent the most likely interaction processes between Tm^{3+} ions in the Tm : Y_2O_3 films. A more complete description of this process, often observed in trivalent rare earth doped optical materials, can be found in ref. 15 and 16. This process occurs when two ions are close enough to interact and when different energy levels are separated by approximately the same energy. Fig. 11 presents three likely cross relaxation processes: $[^1D_2; {}^3H_6] \rightarrow [^1G_4; {}^3F_4]$, $[^1D_2; {}^3H_6] \rightarrow [{}^3H_4; {}^3F_{2,3}]$ and $[^1G_4; {}^3H_6] \rightarrow [{}^3F_{2,3}; {}^3F_4]$. For instance, the process $[^1D_2; {}^3H_6] \rightarrow [^1G_4; {}^3F_4]$ corresponds to a non-radiative de-excitation of one Tm^{3+} ion from the $^1D_2$ level ($^1D_2 \rightarrow {}^1G_4$ transition), and simultaneously the excitation of a second Tm^{3+} ion from the fundamental $^3H_6$ level to the $^3F_4$ level ($^3H_6 \rightarrow {}^3F_4$ transition). Such Tm^{3+}–Tm^{3+} interactions are characterized by a non-exponential behavior in the decay profiles. These interactions are stronger when the thulium ions are close together, *i.e.* when the thulium concentration in the film is high, and so reduce the fluorescence quantum efficiency in the visible range.

In conclusion, to maintain a good quantum efficiency of the emission in the visible range, Tm^{3+}–Tm^{3+} interactions should be reduced and therefore a thulium concentration of lower than 3% is required.

Summary

PLD enables the growth of crystalline Y_2O_3 and Tm : Y_2O_3 thin films, which present a smooth surface morphology and a

good texture whatever the substrates used (Si, MgO and YSZ). We have demonstrated that the crystalline quality depends on the substrate and on the oxygen pressure. In particular, epitaxial growth of Y_2O_3 films of a very high crystalline quality could be achieved on YSZ under vacuum. Thulium doped Y_2O_3 films show visible luminescence results very similar to those obtained on bulk crystalline materials. Luminescence studies in the IR region are currently in progress.

Acknowledgments

This work was supported by the French government (CNRS GDR 86). The authors wish to express their thanks to Dr A. Kahn-Harari, W. Seiler and M. Morcrette for their help during experiments.

References

1 Y. Guyot, R. Moncorgé, L. D. Merkle, A. Pinto, B. McIntosh and H. Verdun, *Opt. Mater.*, 1996, **5**, 127.
2 R. N. Sharma, T. Lakshami and R. C. Rastogi, *Thin Solid Films*, 1991, **199**, 1.
3 K. Onisawa, M. Fuyama, K. Tamura, K. Taguchi, T. Nakayama and Y. Ono, *J. Appl. Phys.*, 1990, **68**, 719.
4 W. M. Cranton, D. M. Spink, R. Stevens and C. B. Thomas, *Thin Solid Films*, 1993, **226**, 156.
5 S. C. Choi, M. H. Cho, S. W. Whanghbo, C. N. Whang, S. B. Kang, S. I. Lee and M. Y. Lee, *Appl. Phys. Lett.*, 1997, **71**, 903.
6 S. Zhang and R. Xiao, *J. Appl. Phys.*, 1998, **83**, 3842.
7 S. L. Jones, D. Kumar, R. K. Singh and P. H. Holloway, *Appl. Phys. Lett.*, 1997, **71**, 404.
8 K. G. Cho, D. Kumar, D. G. Lee, S. L. Jones, P. H. Holloway and R. K. Singh, *Appl. Phys. Lett.*, 1997, **71**, 3335.
9 K. G. Cho, D. Kumar, P. H. Holloway and R. K. Singh, *Appl. Phys. Lett.*, 1998, **73**, 3058.
10 A. Diening, B. M. Dicks, E. Heumann, J. P. Meyn, K. Petermann and G. Huber, *Adv. Solid State Lasers*, 1997, **194**, 10.
11 P. H. Haumesser, J. Théry, P. Y. Daniel, A. Laurent, J. Perrière, R. Gomez-San Roman and R. Perez-Casero, *J. Mater. Chem.*, 1997, **7**, 1763.
12 O. Guillot-Noël, R. Gomez-San Roman, J. Perrière, J. Hermann, V. Graciun, C. Boulmer-Leborgne and P. Barboux, *J. Appl. Phys.*, 1996, **80**, 1803.
13 L. R. Doolittle, *Nucl. Instrum. Methods B*, 1985, **9**, 344.
14 M. J. Weber, *Phys. Rev.*, 1968, **171**, 283.
15 A. A. Kaminskii, in *Lasers Crystals*, Springer Verlag, Berlin, Heidelberg, New York, 2nd edn., 1981, p. 361.
16 N. Britos, A. M. Lejus, B. Viana and D. Vivien, *Eur. J. Solid State Inorg. Chem.*, 1995, **32**, 415.

Paper a904710g